Structural and optical investigation of nonpolar *a*-plane GaN grown by metal–organic chemical vapour deposition on *r*-plane sapphire by neutron irradiation*

Xu Sheng-Rui(许晟瑞)†, Zhang Jin-Feng(张金风), Gu Wen-Ping(谷文萍), Hao Yue(郝 跃), Zhang Jin-Cheng(张进成), Zhou Xiao-Wei(周小伟), Lin Zhi-Yu(林志宇), and Mao Wei(毛 维)

National Key Laboratory of Fundamental Science for Wide Band-Gap Semiconductor Technology, School of Microelectronics, Xidian University, Xi'an 710071, *China*

(Received 16 June 2011; revised manuscript received 12 July 2011)

Nonpolar $(11\bar{2}0)$ *a*-plane GaN films are grown by metal–organic chemical vapour deposition (MOCVD) on *r*-plane $(1\bar{1}02)$ sapphire. The samples are irradiated with neutrons under a dose of 1×10^{15} cm^{-2}. The surface morphology, the crystal defects and the optical properties of the samples before and after irradiation are analysed using atomic force microscopy (AFM), high resolution X-ray diffraction (HRXRD) and photoluminescence (PL). The AFM result shows deteriorated sample surface after the irradiation. Careful fitting of the XRD rocking curve is carried out to obtain the Lorentzian weight fraction. Broadening due to Lorentzian type is more obvious in the as-grown sample compared with that of the irradiated sample, indicating that more point defects appear in the irradiated sample. The variations of line width and intensity of the PL band edge emission peak are consistent with the XRD results. The activation energy decreases from 82.5 meV to 29.9 meV after irradiation by neutron.

Keywords: GaN, neutron, nonpolar, photoluminescence

PACS: 78.55.Cr, 73.61.Ey **DOI:** 10.1088/1674-1056/21/2/027802

1. Introduction

Nonpolar GaN and its alloys have attracted increasing attention for their applications in optoelectronic devices because conventional *c*-plane III-nitride quantum well has a large polarization electric field. The internal electric field, in quantum wells for instance, causes spatial separation of electron and hole wave functions and reduces recombination rate and possibly internal quantum efficiency. This phenomenon is known as the quantum-confined Stark effect.[1−3] To eliminate the internal polarization fields, group-III nitride layers have been recently grown on nonpolar planes, such as *a*- or *m*-plane. In this case, there is no polarization field perpendicular to the layer interface, because the polar *c*-axis lies within the growth plane.[4] It is well known that irradiation of high-energy particles, such as neutrons and electrons, can induce structural defects in semiconductors. And the investigation of irradiation-induced effects on the material properties of group III-nitrides may also provide an insight into the microscopic nature of intrinsic and radiation-induced defects. In the past few decades, there have been many reports on the irradiation-induced defects in *c*-plane GaN. The device operation will be affected by deep level defects, which act as carrier compensation centres.[5−7] However, none of the studies has dealt with the effects of neutron irradiation on the microstructural and optical properties of *a*-plane GaN thin films.

In this paper, we report on neutron irradiation-induced defects and their effects on the morphology and photoluminescence (PL) spectrum. It is found that the full width at half maximum (FWHM) of the PL spectrum of irradiated *a*-plane GaN film increases greatly compared with that of the unirradiated *a*-plane GaN film. The atomic force microscopy (AFM) shows deep surface hole is observed after irradiation. High resolution X-ray diffraction (HRXRD) shows the irradiation deteriorates the crystal quality.

*Project supported by the National Key Science and Technology Special Project, China (Grant No. 2008ZX01002-002), the Major Program and State Key Program of the National Natural Science Foundation of China (Grant Nos. 60890191 and 60736033), and the Fundamental Research Funds for the Central Universities, China (Grant No. JY10000904009).

†Corresponding author. E-mail: shengruixidian@126.com

© 2012 Chinese Physical Society and IOP Publishing Ltd

2. Experimental procedure

Growth of a-plane GaN films was achieved on r-plane $(1\bar{1}02)$ sapphire substrates using a cold-wall showerhead metal–organic chemical vapour deposition (MOCVD) system. After being chemically cleaned, r-plane sapphire substrates were loaded into the chamber. Hydrogen was used as the carrier gas and triethylgallium, trimethylaluminium and ammonia (NH_3) were used as source reactants. A low temperature AlN (LT-AlN) nucleation layer of 20 nm in thickness, a high-temperature AlN (HT-AlN) layer of 100 nm in thickness and a high-temperature AlN (8-nm thick)/AlGaN (12-nm thick) superlattices (SLs) with ten periods were grown at 610 °C, 1050 °C, and 1020 °C, respectively. After buffer layer growth, a 1.5-μm thick a-plane GaN epitaxial layer was grown.[1,4] The sample was irradiated with neutrons under a dose of 1×10^{15} cm^{-2}. Annealing was carried out at room temperature for 20 h in air.

The HRXRD was performed using a Bruker D8-discover system equipped with Ge (220) monochromator and channel-cut analyzer, delivering a pure CuKα line of wavelength $\lambda = 0.15406$ nm. Surface morphologies of samples were characterized by the AFM using Agilent 5500 scanning probe system. The PL measurements were carried out using the 325-nm line of an He–Cd laser. The samples were held in a helium closed-circuit cryostat in a temperature range from 20 K to 300 K. The luminescence was dispersed using a 0.5-m monochromator and detected using a CCD.

3. Results and discussion

Figure 1 shows the measured HRXRD results of the as-grown and the irradiated a-plane GaN films. As we know that the growth of nitride films on foreign substrates typically leads to the presence of built-in anisotropy strain, which is due to the differences in lattice parameter and thermal expansion coefficient between films and substrates. Furthermore, the growth rate along the c direction is much higher than that along the m direction and so the pleat morphology comes forth and produces the anisotropy.[8,9] The XRD rocking curves (XRC) of symmetric reflection measured in different azimuth angles show generally higher FWHM for the irradiated sample and a stronger anisotropy, indicating deteriorated crystal quality due to neutron irradiation. The AFM images of the as-grown sample and the irradiated sample are given in Fig. 2. Compared with the irradiated sample, the as-grown sample has a superior surface quality and less surface pits that should be associated with dislocations. For irradiated sample, it has an anisotropic surface morphology, which is typically observed in the a-plane as-grown GaN but not shown here, owing to the bombardment of high-energy particles.

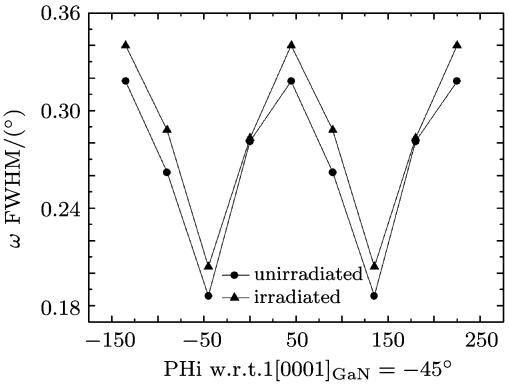


Fig. 1. Azimuth angle dependences of the FWHM of the $(11\bar{2}0)$ rocking curves (XRC) for heteroepitaxially grown a-plane GaN films, unirradiated and irradiated by neutrons.

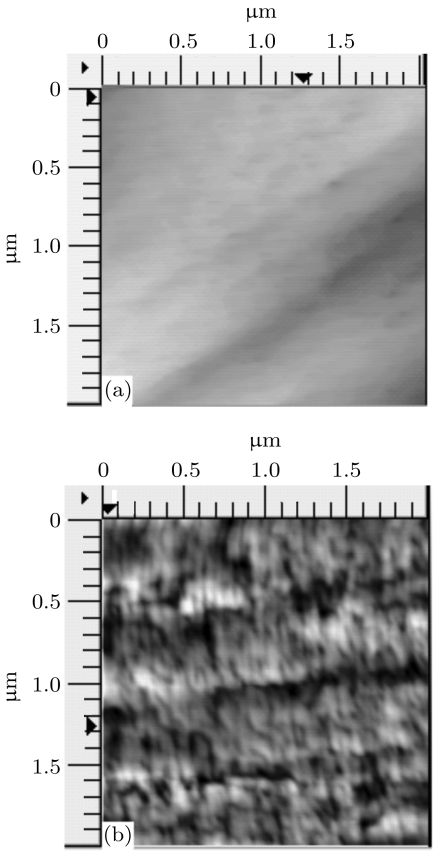


Fig. 2. 2 μm × 2 μm surface morphologies of the as-grown (a) and irradiated (b) samples from AFM.

The peak broadening of XRD is attributed mainly to the nonuniform strained regions near the lattice defects and also to the contributions from instrumental and thermal broadening. The strain broadening of XRD diffraction peak is proportional to the length of

the scattering vector which results in Gaussian broadening; while the size effect has an exponential correlation function leading to Lorentzian broadening.[10] The peak shape analyses of XRD are based on the separation between the Gaussian and the Lorentzian broadening using Pseudo–Voigt function[10,11]

$$fL(x) + (1 - f)G(x), \tag{1}$$

where

$$L(x) = \frac{2A}{\pi} \frac{\beta}{4(x - x_c)^2 + \beta^2}, \tag{2}$$

$$G(x) = \frac{1}{\beta}\sqrt{\frac{\pi}{2}} \exp\left(\frac{-2(x - x_c)^2}{\beta^2}\right). \tag{3}$$

Here, β denotes the FWHM of XRD, when the incident X-ray beam is parallel to the [0001] direction, f represents the Lorentzian shape function, x_c refers to the peak position of XRC, A means the area of the XRC.

In the as-grown and irradiated a-plane samples both Lorentzian and Gaussian broadenings are observed, which shows that the two kinds of defects are present in these samples. The dislocations cause the Lorentzian broadening and the point defects induce the Gaussian broadening. The as-grown sample and the neutron-irradiated sample are fitted shown in Fig. 3 and analysed using methods described earlier and the extracted values are listed in Table 1. After irradiation the Lorentzian component decreases from 0.558 to 0.517, which means that the irradiated sample has more point defects than the as-grown sample. A decrease of β from 0.205 to 0.184 indicates damage after irradiation.

Carrier removal is generally associated with the trapping of majority carriers by structural defect. It is well known that the irradiation of high-energy particles can induce structural defects in semiconductors. To further investigate the crystal structure of the irradiated a-plane GaN, the PL spectra of the samples unirradiated and irradiated by neutrons were measured and their results at 20 K are shown in Fig. 4, where three emission peaks at about 3.474 eV, 3.419 eV, and 3.289 eV can be observed. The 3.474 eV peak is a combination of the free exciton and donor bound exciton transitions. The PL peak at 3.419 eV is most probably due to the recombination of carriers/excitons bound and stacking faults. The 3.289 eV peak is caused by donor–acceptor pair (DAP) emission recombination, which is similar to other results reported in Refs. [12] and [13]. The three PL peaks of the as-grown sample and the irradiated sample come from the same origin. However, the FWHM, the intensity and the position of the peak change after irradiation.

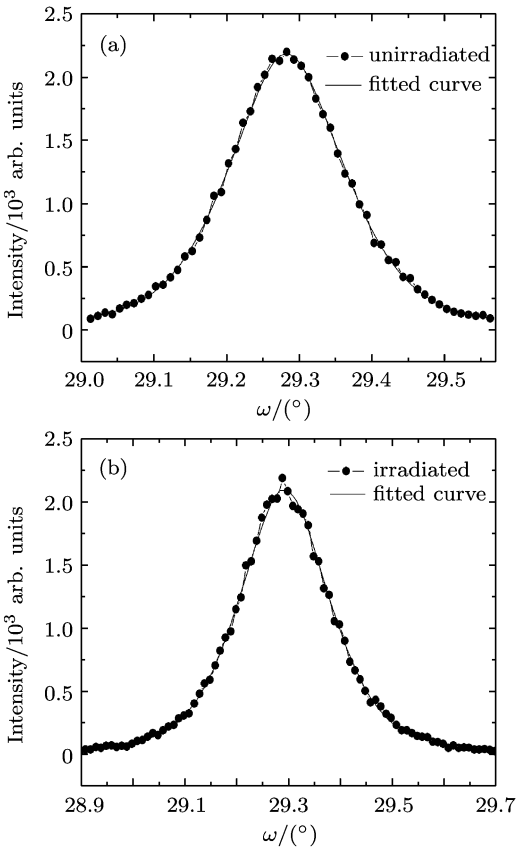


Fig. 3. Pseudo-Voigt function fitting for the as-grown (a) and the irradiated a-plane (b) GaN samples.

To further clarify the PL mechanism of the irradiated sample, temperature dependent PL spectrum is taken from 20 K to 300 K at an excitation power of 30 mW. The wavelength shifts of the exciton peak at about 3.474 eV from 20 K to 300 K are given in Fig. 5, where the peak positions at 20 K are the reference position. For each of the two samples, the peak

Table 1. Parameters extracted from Pseudo-Voigt function fitting of the XRC of the as-grown and irradiated samples.

Samples	FWHM (β)	f (weight of Lorentzian function)	A (area)	x_c (position of ω)
As-grown	0.169	0.558	522	29.28
Irradiated	0.184	0.517	541	29.29

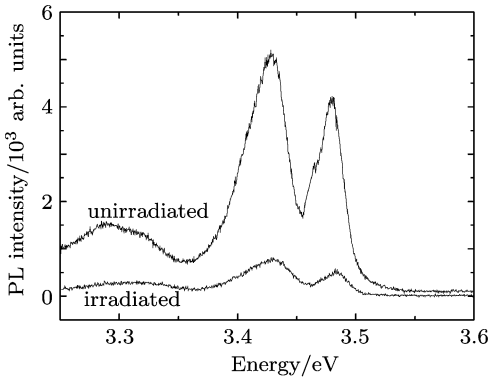


Fig. 4. PL results measured at 20 K for the sample before and after irradiation.

shift of exciton peak varies as a function of temperature from 20 K to 300 K, which exhibits a continuous redshift. But the total redshift value of the as-grown sample is 8.4 meV and that of the irradiated a-plane GaN is 59.5 meV. Figure 6 summarizes the FWHMs of exciton peak for the two samples at different temperatures. The FWHM of the PL spectrum of the irradiated sample is larger than that of the as-grown sample. The PL intensity of the irradiated sample is much lower than that of the as-grown sample. The normalized PL intensities each plotted as a function of $1/T$ for the as-grown and irradiated GaN films are shown in Fig. 7. It is well known that both the peak intensity and FWHM of the PL spectrum from a sample are closely related to its crystal quality. The broadening of the PL peak and the reduction of intensity for the irradiated film indicate that the extent of structural disorder increases and the crystal quality deteriorates. The result of the PL spectrum is consistent with the result of the FWHM of the XRD.

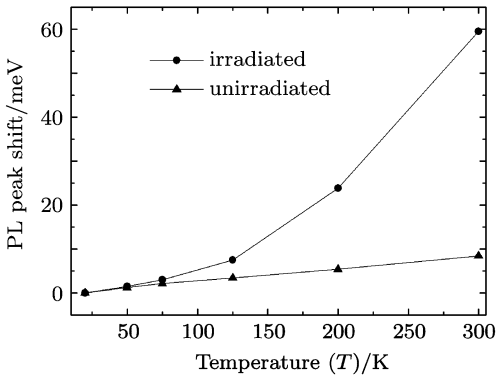


Fig. 5. Wavelength shifts of the exciton peak varying with temperature from 20 K to 300 K for the films irradiated and unirradiated by neutrons.

It has been reported that several defects such as V-defects, stacking faults and dislocations can be formed in GaN films, resulting in deterioration in the

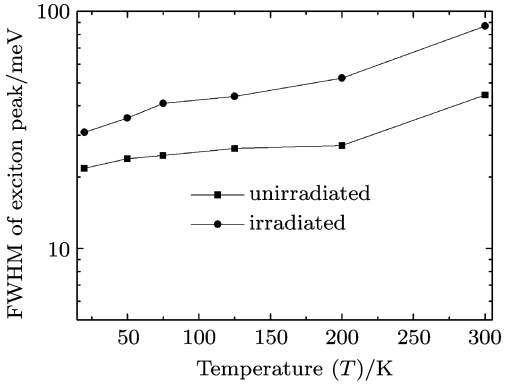


Fig. 6. FWHMs of the exciton peak varying with temperature from 20 K to 300 K for the films irradiated and unirradiated by neutrons.

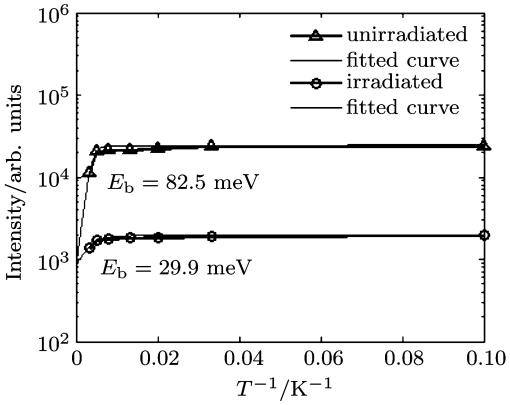


Fig. 7. Normalized PL intensities each as a function of $1/T$ for the samples unirradiatted and irradiated by neutrons.

structural and optical properties of material. Consequently, with neutron irradiation, a large number of defects may exist in the a-plane GaN sample. Photogenerated carriers will be easily trapped by high-density nonradiative centres before they reach the potential minimum. Thus the activation energy must be lower than that of the as-grown sample. The experimental temperature-dependent PL data were fitted by Arrhenius equation to investigate the carrier behaviour,[14,15]

$$I(T) = \frac{I_{\rm O}}{1 + a\exp(-E_{\rm a}/K_{\rm B}T) + b\exp(-E_{\rm b}/K_{\rm B}T)}, \tag{4}$$

where $I(T)$ is the temperature-dependent PL intensity, $I_{\rm O}$ is the PL intensity at 20 K, $K_{\rm B}$ is Boltzmann's constant, a and b are the rate constants and $E_{\rm a}$ and $E_{\rm b}$ are the activation energies for two different nonradiative channels, which can be distinguished according to the low temperature and the high temperature regions.[15] As expected, the activation energy decreases from 82.5 meV to 29.9 meV after being irradiated by neutron.

4. Conclusions

Nonpolar $(11\bar{2}0)$ a-plane GaN films are grown on r-plane $(1\bar{1}02)$ sapphire substrates by MOCVD. The samples irradiated with neutrons under a dosage of 1×10^{15} cm^{-2} are investigated using AFM, HRXRD and PL spectra Pseudo-Voigt function is used to separate the Gaussian broadening from the Lorentzian broadening. Lorentzian type broadening is more in the as-grown sample than in the irradiated sample. As a result more point defects appear in the irradiated sample. In addition, the PL spectrum reveals that the nonpolar as-grown a-plane GaN film has the lower activation energy, which is associated with the dislocations formed in the irradiated process.

References

[1] Xu S R, Hao Y, Zhang J C, Zhou X W, Cao Y R, Ou X X, Mao W, Du D C and Wang H 2010 *Chin. Phys.* B **19** 107204

[2] Zhang J F, Xu S R, Zhang J C and Hao Y 2011 *Chin. Phys.* B **20** 057801

[3] Imer B, Wu F, Speck J S and DenBaars S P 2007 *J. Cryst. Growth* **306** 330

[4] Xu S R, Hao Y, Zhang J C, Zhou X W, Yang L A, Zhang J F, Duan H T, Li Z M, Wei M, Hu S G, Cao Y R, Zhu Q W, Xu Z H and Gu W P 2009 *J. Cryst. Growth* **311** 3623

[5] Wang R X, Xu S J, Fung S C, Beling D, Wang K, Li S, Wei Z F, Zhou T J, Zhang J D, Huang Y and Gong M 2005 *Appl. Phys. Lett.* **87** 031906

[6] Kuriyama K, Tokumasu T, Takahashi J, Kondo H and Okada M 2002 *Appl. Phys. Lett.* **80** 3329

[7] Polyakov A Y, Smirnov N B, Govorkov A V, Markov A V, Pearton S J, Kolin N G, Merkurisov D I and Boiko V M 2005 *J. Appl. Phys.* **98** 033529

[8] Moram M A, Johnston C F, Hollander J L, Kappers M J and Humphreys C J 2009 *J. Appl. Phys.* **105** 113501

[9] Koziorowsk J S, Dimitrakopulos G P, Sahonta S L, Tsiakatouras G, Georgakilas A and Ph Komninou 2008 *Appl. Phys. Lett.* **93** 021910

[10] Sathish N, Dhamodaran S, Pathak A P, Krishna M G, Khan S A, Avasthi D K, Pandey A, Muralidharan R, Li G and Jagadish C 2007 *Physics Research* B **256** 281

[11] Lee S R, West A M, Allerman A A, Waldrip K E, Follstaedt D M, Provencio P P, Koleske D D and Abernathy C R 2005 *Appl. Phys. Lett.* **86** 241904

[12] Netzela C, WernickeT, Zeimer U, Brunner F, Weyers M and Kneissl M 2008 *J. Cryst. Growth* **310** 8

[13] Özgür Ü, Ni X, Fu Y, Morkoc H and Everitt H O 2006 *Appl. Phys. Lett.* **89** 262117

[14] Chiu C H, Kuo S Y, Lo M H, Ke C C, Wang T C, Lee Y T, Kuo H C, Lu T C and Wang S C 2009 *J. Appl. Phys.* **105** 063105

[15] Cho H K, Lee J Y, Kim C S and Yang G 2001 *J. Electron. Mater.* **30** 1348